The problem of capturing marginality in model reductions of turbulence

C Gillot, G Dif-Pradalier, Y Sarazin, C Bourdelle, A Bañón Navarro, Y Camenen, J Citrin, A Di Siena, X Garbet, Ph Ghendrih, et al.

The Problem of Capturing Marginality in Model Reductions of Turbulence

C. Gillot,[1] G. Dif-Pradalier,[1,*] Y. Sarazin,[1] C. Bourdelle,[1] A. Bañón Navarro,[2] Y. Camenen,[3] J. Citrin,[4] A. Di Siena,[2] X. Garbet,[1] Ph. Ghendrih,[1] V. Grandgirard,[1] P. Manas,[1] and F. Widmer[3]

[1] *CEA, IRFM, F-13108 Saint-Paul-lez-Durance, France*
[2] *Max Planck Institute for Plasma Physics, Boltzmannstr. 2, 85748 Garching, Germany*
[3] *Aix-Marseille Université, CNRS PIIM, UMR 7345 Marseille, France*
[4] *DIFFER—Dutch Institute for Fundamental Energy Research, Eindhoven, Netherlands*

(Dated: January 16, 2023)

Reduced quasilinear (QL) and nonlinear (gradient-driven) models with scale separations, commonly used to interpret experiments and to forecast turbulent transport levels in magnetised plasmas are tested against nonlinear models without scale separations (flux-driven). Two distinct regimes of turbulence –either far above threshold or near marginal stability– are investigated with Boltzmann electrons. The success of reduced models especially hinges on the reproduction of nonlinear fluxes. Good agreement between models is found above threshold whilst reduced models would significantly underpredict fluxes near marginality, overlooking mesoscale flow organisation and turbulence self-advection. Constructive prescriptions whereby to improve reduced models is discussed.

Introduction – Fusion plasmas display the property, common in dynamical systems that upon surpassing a critical threshold, an instability may promptly build up, inducing large fluxes which deplete the driving gradients and inhibit the instability. Background gradients thus hover in the vicinity of nonlinear *near marginal* thresholds [1]. Many strategies have been devised in modelling to mimic natural processes. All are not equivalent and different choices may critically affect the nature of computed statistical equilibria.

Forcing-dependent steady-states have indeed long been observed in a variety of systems. Systems with long-range interactions, either controlled in energy or in temperature display different equilibria [2, 3]. Swirling flows controlled through either imposed torque or imposed velocity display distinct steady states, as well as different dynamical regimes [4]. In magnetised fusion plasmas, auxiliary heating and current drive force the system out of equilibrium through a constant flux. Mimicking nature, "flux-driven" (FD) forcing adiabatically imparts a volumetric flux to the system whose gradients self-consistently adapt, leading to the observation of large-scale transport events such as avalanches [5–11], secondary nonlinear structures such as zonal mean flows [12, 13] or tertiary patterns such as staircases [14–19]. Such observations are absent or impaired when the system is driven through a body force, which amounts to imposing fixed mean gradients. This "gradient-driven" (GD) strategy is widely used in direct numerical computations for it is computationally efficient. It indeed enforces, with respect to the FD approach, spatial and temporal scale separations between equilibrium and fluctuations and solves for the fluctuations only.

Known differences between FD and GD frameworks have been documented [17, 18, 20] and related aspects have been discussed in several reviews [21–23]. Whether these are of practical incidence in fusion-relevant configurations is non trivial and these questions are likely exacerbated in near marginal regimes. The matter is important for there are increasing requirements for fast, reduced, yet reliable models to explore the vast parameter space of magnetised plasma turbulence, interpret experimental results and forecast future large experiments such as ITER. Currently, the more advanced reduced models are based on quasilinear theory (QLT) [24–26]. With the advent of machine learning techniques, the ubiquitous closure problem of QLT is approached through data-driven techniques that use large-scale databases of gyrokinetic gradient-driven computations. Systematic shortcomings, if any, within these reference GD strategies are thus likely to be carried over to the reduced models. Comprehensive understanding of discrepancies between first-principles FD, GD and quasilinear approaches is thus important and timely, and the topic of this manuscript.

To this end, we confront reference results from nonlinear FD gyrokinetics using the Gysela framework [27] to state-of-the-art GD nonlinear gyrokinetics and GD quasilinear calculations, using respectively Gkw [28] and QuaLiKiz [29, 30]. We further complement

the study with a twofold confrontation with the QL transport framework of QuaLiKiz–Jetto and with the nonlinear local transport framework of Gene–Tango. In these computations, $N_{r,\mathrm{eval}}$ instances of QuaLiKiz or Gene [31] locally compute at various radii $r_{\mathrm{eval},i}$ (with $0 \leq i \leq N_{r,\mathrm{eval}}$) flux-surface-averaged transport coefficients which are passed on to the Jetto [32] or Tango [33] one-dimensional integrated modelling suites and used to evolve profiles through flux-driven transport equations. After a transport timescale, new local values at each $r_{\mathrm{eval},i}$ location from the evolved profiles are fed to local QuaLiKiz or Gene and the process loops. In practice $N_{r,\mathrm{eval}} = 50$ for QuaLiKiz–Jetto and $N_{r,\mathrm{eval}} = 9$ for Gene–Tango.

Main results are: (i) steady-state predictions of fluxes moderately depend on the nature of forcing *well above nonlinear threshold*; (ii) *near marginality* however, nonlinear and quasilinear GD models sizeably underpredict turbulent heat transport. Under a driving flux, profiles display 'stiffness', i.e. hover in the vicinity of their near-threshold flux-matching values. Large, hot devices such as ITER are expected to be stiff due to the temperature dependence of the gyroBohm heat flux scaling, making near marginality a regime which models must confront. Proximity to nonlinear thresholds implies additional complexity as it favours secondary pattern formation and mesoscale organisation. Despite this additional complexity, (iii) the underlying assumptions of QLT hold well across nonlinear regimes. We show that transport underprediction rather stems from the *choice of closure*, i.e. the *nonlinear saturation rule*. This work stresses the relevance of QLT for model reductions of turbulence whilst providing guidelines whereby reduced models can be improved. The nonlinear and QL approaches tested here are the current workhorse for estimating transport and confinement in turbulent fusion plasmas. This work thus has implications for present-day experimental data analysis and scenario extrapolation for fusion production. Novel saturation rules should strive to incorporate near marginal flux-driven specificities, often dubbed turbulence spreading [11, 34–38], transport nonlocality or staircase organisation.

Frameworks compared – Models are often categorised on being either 'local' (e.g. 'flux-tube') or 'global'. In the local approximation, mean profiles are piecewise constant and boundary conditions periodic; in the global approach, both assumptions are relaxed. There are documented differences between both approaches but for the present discussion, being either local or global is secondary to the fact of being either gradient- or flux-driven. Large scale mean (equilibrium) gradients, as the main source of free energy will of course contribute to driving meso- and micro-scale dynamics. Micro- and meso-scales back react non linearly on the equilibrium profiles via turbulent fluxes. A central question is whether any scale separation (in time and space) exists between turbulence dynamics at micro- and meso-scales on the one hand and equilibrium scales on the other hand. This question is likely all the more critical close to (nonlinear) marginal stability where meso-scale dynamics is more pronounced, memory of smaller scale turbulent activity being 'stored' in meso-scale alteration of equilibrium profiles.

Importantly, in flux-driven frameworks, no scale separation between equilibrium and fluctuations is postulated which implies that the sources and sinks which drive the system out of equilibrium evolve on length scales coarser than that of the turbulence as well as on slow, adiabatic time scales. A continuum of (turbulent) micro- and meso-scales can thus feedback on meso- to macro-scales. In that respect, flux-driven approaches are necessarily global whilst the inverse is not true. One could thus argue that flux-driven and global gradient-driven approaches should render close results *well above threshold*. Closer to (nonlinear) turbulence threshold, *near marginal regimes* are precisely the regimes where global gradient-driven approaches may prove significantly different from flux-driven approaches, for instance through manifestation of Self-Organised Criticality-like phenomena. The curious reader is also referred to e.g. section 4 of Ref.[21], which further illustrates these matters.

Flux-driven Gysela resolves ion Larmor radius scale turbulence and collisional transport in global tokamak geometry, spanning from $r/a = 0$ to $r/a = 1.2$, a being the minor radius of the torus. A centrally peaked heat source drives a deuterium plasma out of equilibrium. For $r/a \geq 1$, a heat sink is progressively applied which allows convergence to a steady temperature profile on energy confinement times. Steady-state and coarse-grained (see below) density n, temperature T, source $\mathcal{S}$ and safety factor q profiles from Gysela are shown in Fig.1. Together with the zonal mean shear shown in Fig.2, they are the reference inputs used to initialise all the other codes. On practi-

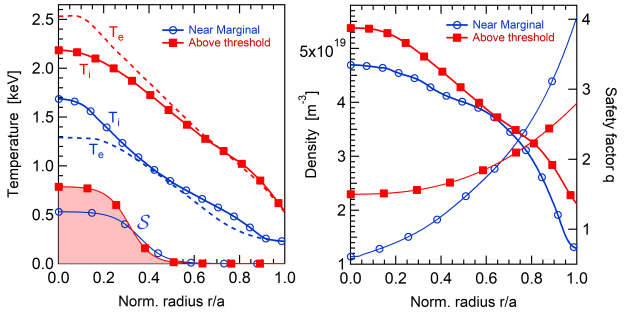

Figure 1. Radial GYSELA profiles of ion and electron temperature, heat source (left), density and safety factor (right) for both 'near marginal' and 'above threshold' cases. The profiles are temporally averaged over $30,000\,\Omega_{ci}$ and radially through sliding windows of $60\,\rho_i$.

cal grounds, the GYSELA profiles need some amount of coarse graining or smoothing before serving as input for either GKW or QUALIKIZ: this is the essence of the scale separation assumption inherent to the gradient-driven approach. In a gradient-driven framework and even more so in the local limit, profiles are indeed required to be smooth below a cut-off radial scale $\ell \leq \ell_c = \max(\lambda_{\rm lin}, \lambda_{\mathbf{E}\times\mathbf{B}})$ whose physics is not included within gradient-driven models. Here $\lambda_{\rm lin} \gtrsim 10 - 20\,\rho_i$ denotes the typical radial extent of unstable growing modes and $\lambda_{\mathbf{E}\times\mathbf{B}} \gtrsim 10\rho_i$ the typical width of mean $\mathbf{E}\times\mathbf{B}$ shear structures [15]. To this end, GYSELA observables are both time averaged at steady-state over $30,000\,\Omega_{ci}$ —which is larger than a typical linear growth time and radially smoothed through sliding windows of $60\,\rho_i$ to smear out flux-driven specificities in the profiles. Here Ω_{ci} is the ion cyclotron frequency. Sliding averages of $20\,\rho_i$ have also been investigated and found insufficient near marginality to smear out memory of meso-scale organisation from the flux-driven framework. This point is further discussed below whilst evoking the role of mean $\mathbf{E}\times\mathbf{B}$ shear.

Gradient-driven models on the other hand (either local or global) exploit to numerical advantage the assumption of a scale separation between a fixed (mean) equilibrium and fluctuations. Sources and sinks are also required in gradient-driven approaches to maintain the system out of equilibrium; the important point is that they depend on the local dynamics of the plasma: maintaining fixed background mean gradients thus acts so as to counter-act part of the natural dynamics of the system (which would naturally relax towards equilibrium), especially hindering spreading and mesoscale dynamics. The appealing semantic contrast between local and global may sometimes cloud the important fact that, especially near marginal stability, what matters is whether these scale separations are postulated or not. Said differently, models are better classified near marginal stability on whether scale separations are postulated or not, whether mesoscale organisation can develop or not and turbulence spreading can occur, unhindered. These questions have been documented both with Boltzmann and kinetic electron responses —see e.g. Fig.2 in Ref.[16], Figs. 5 and 9 in Ref.[17], Figs.10 and 11 in Ref.[18] and Refs.[39, 40]. Inclusion of electron dynamics bears additional physics that will be specifically addressed in a coming work. In the present manuscript, we compare as a first step all approaches with Boltzmann electrons.

Gradient-driven nonlinear GKW exists in both local and global versions; it is here run in its local (flux-tube) setting, solving a limited subset of the whole plasma volume twisting around the torus due to the magnetic shear of the background magnetic equilibrium. GKW is compared to GYSELA at 3 different locations $r/a = 0.3,\ 0.4$ and 0.6. At each of these locations, one first computes the coarse-grained values of the GYSELA profiles (as detailed above) at equilibrium, shown in Figs.1 and 2. These values are used to define the reference background Maxwellian for GKW at each location; GKW then evolves the perturbed distribution function with reference to this fixed background. The resolution chosen for all GKW runs is such that resolved radial and poloidal wavenumbers extend from $(k_\theta\rho_i)_{min} = (k_r\rho_i)_{min} = 0.051$ to $(k_\theta\rho_i)_{max} = 2.6$ and $(k_r\rho_i)_{max}$ is adjusted to match the radial resolution used in GYSELA, i.e. 11.3 for the 'above threshold' case and 8.1 for the 'near marginal' one. This amounts to a radial box size which spans $1/(k_r)_{min} = 2\,\pi \times 19.6\,\rho_i \approx 120\,\rho_i$ at the low field side midplane. A large radial box size of $\sim 120\rho_i$ allows one to avoid unnatural interactions with the periodic boundaries for the GKW computations, in consistency with the local framework, are radially-periodic. GKW thus effectively computes at each location $r/a = 0.3,\ 0.4$ and 0.6 a nonlinear realisation in the local gradient-driven approximation of the dynamics locally expected of the coarse-grained flux-driven GYSELA profiles.

Further reducing model complexity, turbulent

structures are expected with the quasilinear approximation to bear memory in shape and localisation of their linear generation mechanism. They remain radially thin around a reference magnetic surface and only depend on local plasma parameters and on local gradients. This is direct consequence of the assumption which relates the distribution function fluctuations to the potential fluctuations through local equilibrium parameters. This induces, as with the gradient-driven approach, a spatial scale separation between a local turbulent behaviour, and a slower and smoother evolution of the profiles. Quasilinear QuaLiKiz is run here in 2 configurations: in its standalone version, it is inherently local; in its version coupled to the transport code Jetto, the local transport coefficients from QuaLiKiz are used as inputs for transport equations, thus allowing for the equilibrium to evolve on transport timescales whilst retaining the locality and scale separation assumptions on shorter length- and time-scales. QuaLiKiz solves the gyro-kinetic dispersion relation, here with Boltzmann electrons. For efficiency, the analytic distribution response is simplified by computing the shape of the potential fluctuations in the fluid limit [29], while keeping a kinetic treatment of the wave–particle resonance. Stable modes are neglected; unstable modes are accounted for through a double power law in k_θ for the turbulent intensity spectrum. The amount of numerical integrations is limited by performing the resonant velocity integration analytically. The effect of zonal flow shear is modelled by perturbative modification of this response. Extensive benchmarks with local gradient-driven gyrokinetic codes have led to refining the closure for the potential fluctuations [30, 41], calibrated to a database of local nonlinear gyrokinetic simulations akin to those presented here with Gkw.

Finally, two additional series of computations have been performed in 'near marginal' and 'above threshold' settings using the integrated scheme of Gene–Tango. This additional framework complements the Gkw and QuaLiKiz–Jetto approaches: Gene is a gradient-driven local nonlinear gyrokinetic framework akin to Gkw and the transport framework of Tango is similar to Jetto. Comparison between the combined Gene–Tango and QuaLiKiz–Jetto frameworks allows to test (i) the impact of the QL reduction with respect to nonlinear evolution. Since both Gene and QuaLiKiz have scale separations built in their framework, comparison of both approaches to Gysela also allows to specifically assess (ii) the influence of the scale separation assumption. This point is further discussed below and is found to be important near marginal stability.

All 4 approaches can handle complex geometries yet here, for the sake of simplicity, each is set to run in the same simplified toroidal magnetic geometry with circular and concentric flux surfaces $\mathbf{B} = (B_0 R_0/R)[r\mathbf{e}_\theta/qR_0 + \mathbf{e}_\varphi]$, where $\mathbf{e}_\theta$ and $\mathbf{e}_\varphi$ are the unit vectors in the poloidal and toroidal directions, B_0 is the magnetic field on axis, r the minor radius and $R = R_0 + r\cos\theta$ the major radius.

Let us close this section with 2 concluding remarks. First, it is worth emphasising that the impact of the type of forcing on turbulent transport and achievable steady-states is not restricted to numerical simulations. Experimentally, it is well documented in fluids that the statistics of flow states as well as transitions between them may critically depend on the type of forcing applied –e.g. in von Kármán flows either at constant impeller speed or at constant torque [4]. These observations are analogous to respectively the gradient- and flux-driven cases discussed above. Not surprisingly, the difference between both regimes manifests close to transitions between two equilibrium states while disappearing away from the transition. Again, this behaviour is reminiscent of magnetised plasma dynamics near marginal (nonlinear) stability or above threshold.

Last, comes the important question of the nonlinear saturation of turbulence in all 3 approaches. $\mathbf{E}\times\mathbf{B}$ shear has at least two components, a mean part and a fluctuating part which may affect and regulate the system differently, over different timescales and through possibly distinct pumping and damping mechanisms. In Gysela both components are self-consistently computed and act in concert. A radial force balance $E_r - V_T B_P + V_P B_T = \nabla p/ne$ is satisfied throughout the computation [42]. This is not so for QuaLiKiz, Gkw or Gene for which the mean part is unconstrained. It is an input that can be freely imposed in local approaches without breaking constitutive orderings, echoing the fact that the above radial force balance is not required to be satisfied. Gkw and Gene thus only compute the fluctuating $\mathbf{E}\times\mathbf{B}$ shear as part of the nonlinear response. For QuaLiKiz in its standalone version, the mean $\mathbf{E}\times\mathbf{B}$ shear is an input as well and the effect of the fluctuating $\mathbf{E}\times\mathbf{B}$ flows on the saturation of turbulence is part of the closure

scheme, thus approximated from local nonlinear gyrokinetics. In the QuaLiKiz–Jetto framework this must be slightly nuanced: (*i*) the transport equation leads to an evolving pressure gradient; (*ii*) toroidal velocity V_T can either be prescribed from measurements or self-consistent from the momentum transport equation including external torque and QuaLiKiz momentum transport and (*iii*) poloidal velocity V_P is evaluated from the neoclassical transport model Nclass [43]. The QuaLiKiz–Jetto interface then estimates E_r through radial force balance. From there comes the perpendicular velocity shear input into QuaLiKiz at each radial grid point. Note that a similar procedure exists in the Gene–Tango interface but has not been used for the present study. Note as well that even with this consistent evaluation of radial force balance not all relevant flows are taken into account in these approaches and in particular no structuring at mesoscales can occur due to the built-in scale separation assumptions. In the case of QuaLiKiz there are also additional missing intrinsic rotation or turbulence-generated zonal flows effects.

In the present manuscript, we focus on testing consequences of constitutive assumptions in the models and therefore choose to impose in Gkw and QuaLiKiz the local values of mean $\mathbf{E}\times\mathbf{B}$ shear from Gysela. One could also ask for a complementary approach and e.g. only consider the self-consistent fluctuating $\mathbf{E}\times\mathbf{B}$ shear from nonlinear Gkw or Gene or the shear effectively allowed in QuaLiKiz through the choice of closure and ask how this would compare to Gysela. This is done in the Gene–Tango framework where the mean $\mathbf{E}\times\mathbf{B}$ shear from Gysela is not imposed and only the fluctuating $\mathbf{E}\times\mathbf{B}$ shear from Gene is included. A comprehensive discussion of these issues is beyond the scope of the present work but one would expect discrepancies between models to be especially visible near marginal stability. Indeed, the possibility to self-consistently evaluate the mean $\mathbf{E}\times\mathbf{B}$ shear is directly connected to the role of mesoscale organisation and only fully present in flux-driven Gysela. To illustrate this point, let us emphasise that computed fluxes from Gkw and especially from QuaLiKiz show significant sensitivity near marginality to imposed levels of mean $\mathbf{E}\times\mathbf{B}$ shear (within one standard deviation) when mean $\mathbf{E}\times\mathbf{B}$ shear profiles from Gysela are only smoothed over $20\,\rho_i$ (approximately twice the mean flow width or the width of mean profile corrugations [18]). This sensitivity is much less pronounced with the $60\,\rho_i$ radial smoothing of the Gysela profiles reported here. This is certainly illustrative of the important role that mean $\mathbf{E}\times\mathbf{B}$ shear plays in FD approaches near marginality. Conversely, the fact that QuaLiKiz–Jetto and Gene–Tango provide comparable results with the $60\,\rho_i$ radial smoothing despite different imposed levels of mean $\mathbf{E}\times\mathbf{B}$ shows that the strong coarse graining applied to Gysela effectively minimises discrepancies with the other approaches. The near marginal flux underprediction which we report below is thus likely significant and possibly a lower-bound estimate of actual differences.

This question of a consistent evaluation of mean $\mathbf{E}\times\mathbf{B}$ shear/of mesoscale organisation is certainly an interesting one for prospective gradient-driven computations which would aim to provide quantitative answers for new/untested plasma configurations for which there is no a priori "ground truth" (experimental or flux-driven). To try to mitigate this problem local frameworks are thus increasingly coupled to transport equations, which provide a step towards a more self-consistent coupling between mean and fluctuations. In that respect, the lingering discrepancy between Gysela on the one hand and both QuaLiKiz–Jetto and Gene–Tango on the other hand, visible in Fig.4-(c), is certainly indicative of the fact that coupled models where the turbulence model is yet based on a scale separation still miss part of the dynamics near marginal stability. This important observation certainly calls for further studies on the matter, whilst especially relaxing the assumption of Boltzmann electrons.

Two distinct regimes – Two paradigmatic simulation regimes are considered in the electrostatic regime with Boltzmann electrons. Both cases are run in the so-called "local limit" [44], at $\rho_* = \rho_i/a \leq 1/250$, where comparison to local Gkw is fair. Coarse-grained (see above) radial profiles of normalised tem-

Case	$\rho_{\star,50}$	R/a	$\nu_{\star,50}$	$(q_{50}\,;\,q_{95})$	$\tau = T_i/T_e$
near marginal	1/250	3.2	0.24	(1.4 ; 4.0)	$1 < \tau < 1.3$
above thresh.	1/350	6	0.02	(1.7 ; 2.8)	$0.9 < \tau < 1$

Table I. Main plasma parameters in considered cases. Subscripts $_{50}$ and $_{95}$ respectively denote parameter values estimated at locations $r/a = 0.5$ and $r/a = 0.95$.

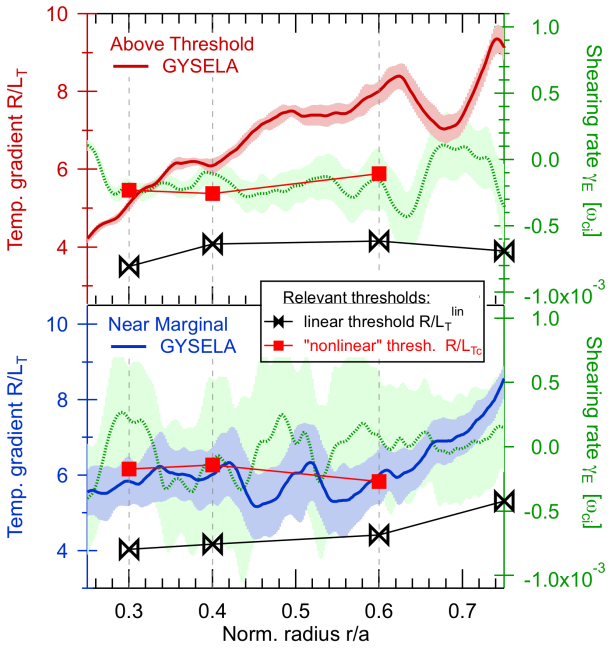

Figure 2. Radial profiles of normalised temperature gradients (blue and red, left axis) and zonal flow shear (green, right axis) for the 'above threshold' (top) and 'near marginal' (bottom) cases. Shaded areas represent temporal standard deviation; black hourglass symbols (⋈) linear instability thresholds $R/L_T^{\rm lin}$ at vanishing $\mathbf{E}\times\mathbf{B}$ shear; red squares (■) nonlinear thresholds R/L_{Tc} estimated by GKW in the local limit, including the GYSELA $\mathbf{E}\times\mathbf{B}$ shear.

perature gradients $R/L_T = -R\partial_r T/T$ and zonal flow shear are plotted in Fig.2 for the 'above threshold' (top) and 'near marginal' (bottom) cases. Shaded areas represent temporal standard variations. The large deviation from the mean shearing rate in the 'near marginal' case (bottom, right axis) results from the meandering of staircases, which have already been reported to play an important role in this regime of parameters [18]. The linear (black hourglass symbols) and nonlinear (red squares) thresholds are discussed in next section. In order to broadly span parameter regimes, main plasma parameters vary significantly between cases, as illustrated in Table I. This choice echoes the fact that parameter space is broad and parsing it is uneasy. A comprehensive discussion of the precise impact of each parameter: $\rho_\star$, aspect ratio R/a, τ,... is a daunting task. We take a first step in this direction and choose to broadly span parameters from the 'near marginal' case to the 'above threshold' case. One wishes thus to minimise the possibility that found conclusions may strongly depend on the precise corner of parameter space that is investigated. Of course the present approach will require to be complemented by further dedicated studies specially focusing on scanning one parameter or the other.

Our choice of parameters in Table I is however not totally random as we have performed with GYSELA extensive aspect ratio (in the range $R/a = 3-10$) and $\rho_\star$ scans (in the range $\rho_\star^{-1} = 190-380$) and found numerically a confinement time scaling law of the form: $\tau_c\,\Omega_{ci} \propto (R/a)^{0.88}\,\rho_\star^{-2.4}$ [45]. The 'near marginal' case has both a larger $\rho_\star$ and a lower aspect ratio than the 'above threshold' case. Given the above scaling, one may expect for the 'near marginal' case a degraded confinement with respect to what would have been obtained should we have run the 'near marginal' profiles with the R/a and $\rho_\star$ parameters of the 'above threshold' case. This is an important point: the parameters chosen for the 'near marginal' case are not such that they strengthen flux-driven specificities. Rather the opposite: beneficial zonal flow activity through mesoscale staircase organisation is indeed observed to be enhanced at smaller $\rho_\star$ values [14], allowing to recover favourable gyro-Bohm-like confinement scaling by taming avalanching/spreading activity through successive staircase steps (see e.g. section 2.4 in Ref.[18]). Anticipating on the following sections, the discrepancy found in the near marginal regime between GYSELA on the one hand and either GKW, QUALIKIZ, QUALIKIZ–JETTO or GENE–TANGO on the other hand strengthens the necessity to further understand and incorporate near marginal physics in reduced gradient-driven or quasilinear models of turbulence.

For each set of local values of the GYSELA parameters, two thresholds are to be distinguished: linear $R/L_T^{\rm lin}$ represents the normalised temperature gradient above which an unstable mode grows, at vanishing $\mathbf{E}\times\mathbf{B}$ shear. The inclusion of self-generated flow shear –nonlinear in essence– introduces a second threshold R/L_{Tc}, indicative of the nonlinear saturation of turbulence [46], in particular by zonal flows. Practically, R/L_{Tc} is computed in local GD frameworks as the minimum local temperature gradient which provides a non-vanishing nonlinear heat flux. It is estimated with GKW through a series of increasing R/L_T nonlinear computations, whilst imposing local $\mathbf{E}\times\mathbf{B}$ shear val-

ues from flux-driven GYSELA. We call 'above threshold' the regime such that $R/L_T^{\rm lin} < R/L_{Tc} \ll R/L_T$, characterised by a static, smooth zonal mean shear $\gamma_E = \partial_r^2\langle\phi\rangle/B$ and subdominant zonal fluctuations. The flux-surface average of the electric potential is $\langle\phi\rangle$, $\tilde{\phi}$ are its fluctuations. We call 'near marginal' regimes such that $R/L_T^{\rm lin} < R/L_T \lessapprox R/L_{Tc}$. Proximity from below to R/L_{Tc} is a hallmark of near marginality, featuring a well-defined staircase pattern of flows and associated temperature corrugations which meanders within the time interval –hence the large shear deviation– and significant avalanching activity [18].

Kubo numbers of order unity – QLT is valid [47] in the low Kubo number limit $K = \tau_{\rm jump}/\tau_{\rm int} < 1$, ratio of a jumping time $\tau_{\rm jump}$ of particles from one turbulent eddy to the next over a nonlinear eddy-particle interaction time $\tau_{\rm int}$. Kubo numbers are estimated from the GYSELA flux-driven data in various ways, summarised in Tab.II. With analogy to incompressible fluids, particles trapped in turbulent convective cells explore eddies in a typical turn-over time given by the local vorticity $\tau_{\rm int}^{\rm trap} \sim B/\langle|\nabla_\perp^2\tilde{\phi}|^2\rangle^{1/2}$. Whilst they undergo this vortical motion they also drift in about $\tau_{\rm jump}^\star \sim L_\theta(eB/\nabla T)$ from one turbulent structure to the next at the typical speed of the local diamagnetic velocity. Alternatively, the slower evolution of the potential field provides a relevant correlation time $\tau_{\rm jump}^{\rm corr}$ for turbulent fluctuations, trade-off between unstable growth and nonlinear saturation. It must be computed as a Lagrangian correlation time, in the co-moving frame of the eddies to correct for the Doppler shift due to turbulence mean rotation and the eddy velocity. We estimate it through image registration, following the toroidal shift between 3-dimensional turbulence snapshots of $\tilde{\phi}$. It is compared to turbulence-driven stochastic transport times of particles which, assuming a diffusive ansatz for $\mathbf{E}\times\mathbf{B}$ fluctuations, drift across eddies in about $\tau_{\rm int}^{{\rm diff},x} = L_x/\langle|\tilde{v}_{E,x}|^2\rangle^{1/2}$, with $x = \{r,\theta\}$ and L_x the transverse correlation lengths computed from GYSELA outputs. Interestingly, employing a Eulerian correlation time would result in severe Kubo number overestimation, locally up to factors of 25.

Particle trapping $K_{\rm trap}$	transverse drifts $\tau_{\rm jump}^\star$	
	eddy turn-over $\tau_{\rm int}^{\rm trap}$	
Random walks $K_{\rm diff}^{\{r,\theta\}}$	Lagrang. correlation time $\tau_{\rm jump}^{\rm corr}$	
	$\mathbf{E}\times\mathbf{B}$ random walk $\tau_{\rm int}^{{\rm diff},\{r,\theta\}}$	

Table II. Five typical wave–particle and turbulent times lead to three Kubo number combinations, shown in Fig.3.

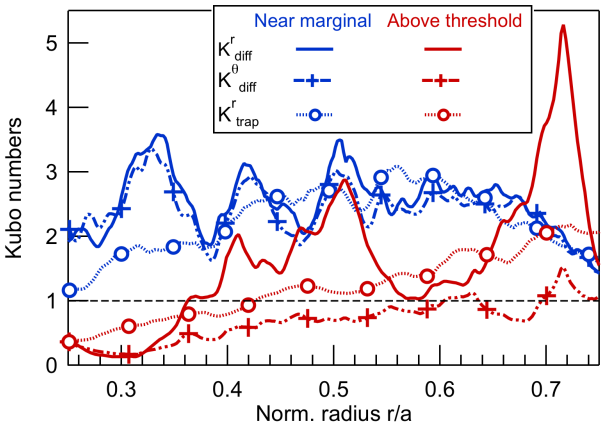

Figure 3. Kubo numbers for the principal nonlinear dynamics in the problem. Plain and plusses: turbulent radial and poloidal $\mathbf{E}\times\mathbf{B}$ velocity effect during a turbulent auto-correlation time. Circles: trapping of particles due to turbulent vorticity during transverse crossing of the turbulent filament.

Three Kubo numbers, combinations of the above nonlinear times are plotted in Fig.3 for both 'above threshold' and 'near marginal' regimes. The various definitions for K, coherent, provide the following picture: (i) on the basis of order unity Kubo numbers, QLT should be marginally valid. Yet, as shown below, key assumptions at the heart of the QLT reduction remain valid throughout nonlinear evolution, which strengthens the case for quasi-linear integrated modelling. Interestingly also, (ii) consistently larger K values near marginality stress the more percolative nature of transport there. Avalanching emerges as a key theme to distinguish between 'above threshold' and 'near marginal' regimes as they likely underpin the larger K values computed near marginality. It is a likely indication that incorporating avalanching and its zonal mean flow regulation may significantly alter transport predictions and improve model behaviour near marginality.

Near marginal heat flux underprediction – Heat fluxes are computed with QUALIKIZ, GKW or GENE from the GYSELA time-averaged steady-state profiles plotted in Figs.1 and 2 with the same degree of approximations (electrostatic & Boltzmann

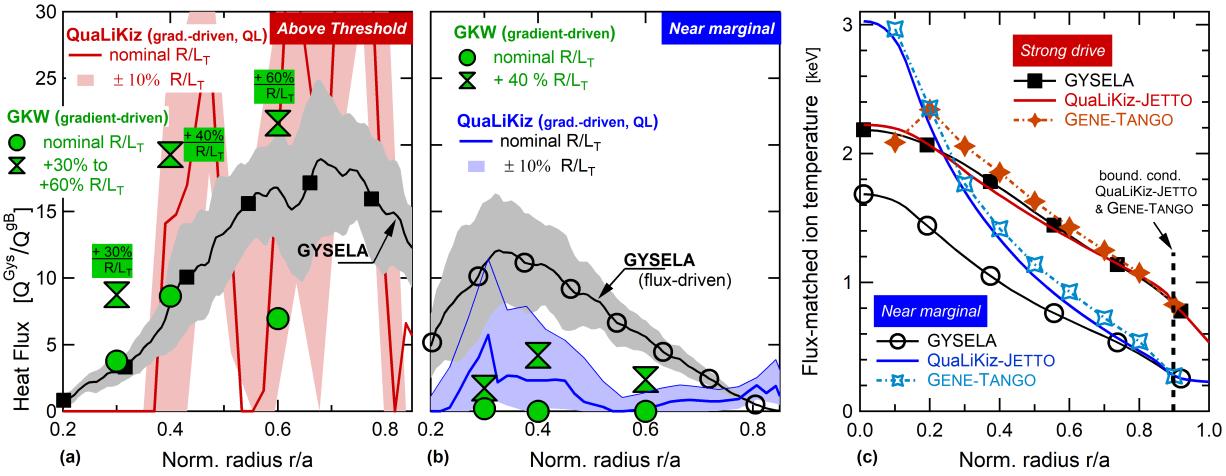

Figure 4. (a) and (b): gradient-driven QuaLiKiz and Gkw heat fluxes confronted to reference flux-driven Gysela flux levels, based on the Gysela profiles of Fig.2 and expressed in gyro-Bohm unit. Gray shaded areas represent a standard deviation of Gysela heat fluxes during the considered time interval, as profiles fluctuate. Red and blue shaded areas represent the sensitivity of QuaLiKiz to these profile variations; the hourglass symbols that of Gkw to a increased input temperature gradients. The reversed approach is followed in panel (c): heat fluxes in QuaLiKiz–Jetto and Gene–Tango are made to match the Gysela reference fluxes; the unknowns are thus the QuaLiKiz–Jetto and Gene–Tango profiles. The remarkable agreement above threshold and large over-prediction of the temperature gradient near marginality are consistent with results in panels (a) and (b). This emphasises model reduction adequacy in 'above threshold' regimes and missing physical ingredients in 'near marginal' regimes.

electrons). All codes have different normalisations, with Gysela e.g. being normalized to $\hat{Q}^{\rm Gys} = Q/(n_0 T_0 v_{Ti0})$ with $v_{Ti0} = (T_0/m_i)^{1/2}$ the ion thermal velocity. In Fig.4–(a) and (b), fluxes from all codes are in the units of $\hat{Q} = \hat{Q}^{\rm Gys}/\hat{Q}^{\rm gB}$, with $\hat{Q}^{\rm gB} = \rho^2_{\star,50}\, a/R$ and values of $\rho_{\star,50}$ and R/a given in Tab.I. Consistent rescaling factors have been applied to QuaLiKiz and Gkw fluxes. Non-axisymmetric (turbulent) contributions to heat fluxes are shown in Fig.4–(a) and (b). Turbulence spreading and profile corrugations, inherent to flux-driven complexity are absent or hindered in all QL or GD approaches. A fair comparison thus requests that the Gysela reference data be significantly coarse-grained before being handed over to Gkw, Gene or QuaLiKiz as input profiles. This smoothing includes the $\mathbf{E}\times\mathbf{B}$ shear profiles. Hence the time averaging over $30,000\,\Omega_{ci}$ and radial smoothing over $60\,\rho_i$ performed on the Gysela observables, as detailed above —to smear out visible flux-driven specificities in the profiles. The stabilising effect of mean zonal flow shear is accounted for in Gkw and QuaLiKiz whilst locally imposing the smoothed reference Gysela mean shear values. In Gene–Tango only the fluctuating $\mathbf{E}\times\mathbf{B}$ shear is included —see discussion above. Sensitivity to gradient fluctuations, inherent to gradient-driven approaches is further assessed by additional scans in R/L_T and $\mathbf{E}\times\mathbf{B}$ shear within one temporal standard deviation of the Gysela profiles.

Without inclusion of $\mathbf{E}\times\mathbf{B}$ shear stabilisation *[i]* QuaLiKiz heat fluxes are overestimated with respect to Fig.4 by over an order of magnitude (not shown here). With the inclusion of shear, *[ii]* at locations of low or vanishing $\mathbf{E}\times\mathbf{B}$ shear and despite the $60\,\rho_i$ smoothing, gradient-driven (standalone) QuaLiKiz commonly displays [subplots (a) and (b)] variations by factors in heat fluxes from one radial position to the next whilst Gkw exhibits much less sensitivity to $\mathbf{E}\times\mathbf{B}$ shear stabilisation. Interestingly, this large sensitivity of QuaLiKiz to shear is mitigated when called within the integrated framework of Jetto [32] to allow for a flux-driven QL profile evolution, driven by a central source that mimics the one of Gysela [subplot (c)]. In the regime above threshold *[iii]* reasonable agreement in computed fluxes is found across fidelity hierarchy. Conversely near marginality, *[iv]*

despite significant smoothing, heat flux discrepancies in Fig.4–(b) are well outside allowed gradient sensitivity and fluctuation 'error' bars. Secular growth of zonal flows in GKW is responsible for the observed large flux underprediction. This echoes previous observations casting concern on near marginal gradient-driven predictions [17]. The soundness of separating fluctuations from mean is thus clearly questioned near marginality.

The conclusions above are further confirmed when comparing FD GYSELA to the FD quasilinear frameworks of QUALIKIZ–JETTO and GENE–TANGO, in the same two regimes. In subplot (c), profiles from QUALIKIZ–JETTO and GENE–TANGO are evolved until heat fluxes match the nonlinear GYSELA reference fluxes. The figure of merit now becomes how close evolved quasilinear or nonlinear profiles are at flux equilibrium with those of GYSELA. Remarkable *[v]* profile agreement is found for both approaches in the 'above threshold' case, which in the case of QUALIKIZ also echoes the agreement in fluxes displayed in panel (a). Near marginality however, *[vi]* a large over-prediction of the temperature is required for both QUALIKIZ–JETTO and GENE–TANGO to carry the same flux as GYSELA. Interestingly, the fact that both quasilinear QUALIKIZ–JETTO and nonlinear GENE–TANGO frameworks provide consistent results illustrates the fact that *[vii]* the QL reduction is not a priori responsible for the observed flux under-prediction in the 'near marginal' regime. A constitutive ingredient is missing in this regime, at least with Boltzmann electrons, which is due to either the local or the gradient-driven approximation. This rather clearly *[viii]* points towards a problem with the scale separation assumption near marginality and gives a workable route for improvement.

Axis for improvement: saturation rules – Flux discrepancies between GYSELA and GKW likely stems from disregarding the feedback of fluctuations on an assumed fixed "equilibrium". This enforces local and single-valued flux–gradient relations, underestimates turbulence spreading, avalanching and mesoscale organisation. All of which contribute to transport, especially near marginality. Discrepancies with QUALIKIZ may either come from violating assumptions central to QLT –linearity of fluctuations– or by inheriting shortcomings akin to those of GKW, through the choice of saturation rules.

To disentangle these questions, we compute in

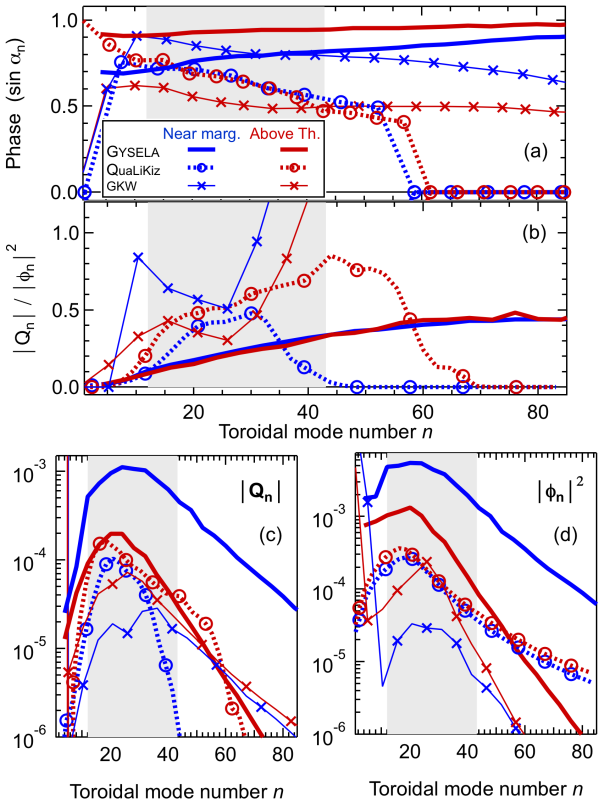

Figure 5. Testing spectral distribution of key fundamental quantities: (a) linear cross-phases, (c) heat flux, (d) saturation rule and (b) their ratio, proxy to the dispersion relation from GYSELA (−), GKW (×) and QUALIKIZ (○), averaged over radial interval $0.3 \leqslant r/a \leqslant 0.7$.

Fig.5, for all three approaches, the complex argument α_n of the n-th Fourier component of the heat flux [panel (a)] –a proxy for the linear cross-phase between electric potential and pressure fluctuations. They depend on the toroidal wave number n labelling each eigenmode which is related to the normalised poloidal wave vector $k_\theta \rho_i$ through: $k_\theta \rho_i = (a/r)\, n\, q\, \rho_\star$. In the present cases, the $n = 25$ toroidal wave number corresponds to, at mid-radius $a/r = 2$: $k_\theta \rho_i = 25{*}1.4{*}2/250 = 0.28$ and $k_\theta \rho_i = 25{*}1.7{*}2/350 \approx 0.24$ for the 'near marginal' and 'above threshold' cases, respectively. In GYSELA, $Q_n^{\rm Gys} = -i|Q_n|e^{i\alpha_n} = \int \hat{v}^r_{E,n} \frac{2}{3} \left(\hat{P}^*_{||,n}/2 + \hat{P}^*_{\perp,n} \right) {\rm d}\theta$, where parallel and transverse components of the pressure and the radial component of the $\mathbf{E} \times \mathbf{B}$ drift are computed from 3D output data. The n-Fourier components of the heat flux

$|Q_n|$ and of the squared potential $|\phi_n|^2$, i.e. the saturation rule are respectively shown in panels (c) and (d). Panel (b) displays their ratio, a proxy for the dispersion relation, sometimes called 'QL flux integrals'.

Clearly, linear cross-phases display reasonable agreement, within factors of 2 and across all regimes. They are not responsible for the flux discrepancies. Factors of disagreement –and avenues of improvement for QL modeling– are essentially twofold: *[i]* 90% of the heat flux is carried by modes $n \in [\![5, 50]\!]$ in the 'above threshold' regime; all approaches provide similar conclusions. Near marginality however, flux is carried in GYSELA and GKW through $n \in [\![5, 70]\!]$, twice the amount of active modes with respect to QUALIKIZ. Furthermore, *[ii]* saturation rules are clearly responsible for much of the observed flux discrepancies. In the 'above threshold' regime, flux spectra agree well [panel (c)] –though this results from a surprising compensation: the potential, or saturation rule [panel (d)] is under-estimated, the dispersion relation [panel (b)] is over-estimated yet heat flux spectra in the 'above threshold' regime are in reasonable agreement. No such compensation occurs near marginality; there severe under-estimation of the potential spectrum is clearly responsible for the under-prediction of fluxes.

Outlook – The success of reduced models especially hinges on the reproduction of nonlinear gyrokinetic fluxes [30]. Flux under-prediction in the dynamically important regime of near marginal stability is thus a matter of importance. At the heart of this paper lies the fact that fkux-driven (FD) and gradient-driven (GD) models provide significantly different flux predictions with Bolzmann electrons close to marginal stability R/L_{Tc}, which underpins basic discrepancies in how nonlinear saturation of turbulence is modelled. This should foster renewed interest in ways to complete quasilinear (QL) or GD models near marginality. The robustness of linear features [48] across fidelity hierarchy and across turbulent regimes is encouraging perspective and provides constructive directions whereby reduced models could be improved.

Discrepancies between the nonlinear frameworks of GYSELA and of both GKW and GENE–TANGO are strong indications that turbulence spreading and mesoscale patterning are in fact central to accurate transport predictions near marginality. Larger Kubo numbers near marginality, as shown in Fig.3 reinforce this point, which is also differently stressed by recent works in the plasma edge [11, 38]. The fact that QUALIKIZ behaves better near marginality than GKW is possibly because the QL closure does not include the long-lived zonal flows that quench transport near marginality in GD approaches [17]. In QUALIKIZ, stable modes are neglected and the turbulent intensity spectrum is fitted [30, 41] onto databases of GD nonlinear computations, similar to those presented here with GKW. With this procedure, QL models inherit the shortcomings of the primitive gradient-driven models onto which they are adjusted. The near marginal transport shortfall in QUALIKIZ indeed largely comes from issues with the QL closure, i.e. the choice of saturation rule and not the QL reduction, *per se*. The QUALIKIZ–JETTO framework provides a step towards coupling fluctuations with mean dynamics. This framework yet emphasises a similar near-marginal flux under-prediction, well reproduced by the similar yet fully nonlinear framework of GENE–TANGO. This is further indication that the leading-order problem is likely the assumption of a scale separation between 'equilibrium' mean scales and fluctuating scales, the latter not being able to feed back onto the former. In the case of QUALIKIZ, this scale separation is inherited from the choice of the saturation rule.

This provides directions for improvement. In physical terms, near marginal regimes require description of transport below or at linear stability and of possible coupling to modes presently predicted as stable in QUALIKIZ. Importantly, it also requires to model the self-advection (spreading) of turbulent domains and the possibility of non-monotonic flux-gradient relations. Several routes can be explored. In the spirit of current frameworks, QL models could be trained on near marginal flux-driven databases such as provided by the likes of GYSELA. This would likely lead to QL closures with regime-dependent turbulent intensity spectra. Alternatively to present closures, QL models could also be coupled to dynamic equations for the turbulence intensity, e.g. in the form of reaction–diffusion [49] or $k - \epsilon$ equations [50], enriching accessible nonlinear dynamics.

The present work provides a framework of understanding. Ongoing studies are concerned with further characterising the 'above threshold' and 'near marginal' regimes [51] when kinetic features of electron dynamics are present. This is important to assess relevance for ITER extrapolations. Electron dy-

namics is indeed known to locally modify turbulence organisation near low order rational surfaces [52] yet, interestingly, key features of near marginal turbulence with Boltzmann electrons (flow patterning, shear effectiveness and staircase organisation) —central here to the 'near marginal' regime— robustly endure in kinetic electron regimes [39].

Acknowledgements – The authors acknowledge stimulating discussions with P.H. Diamond, A. Ashourvan and participants at the 2019 and 2021 "Festival de Théorie" in Aix-en-Provence. This work has been carried out within the framework of the EUROfusion Consortium and was supported by the EUROfusion Theory and Advanced Simulation Coordination (E-TASC) initiative under the TSVV (Theory, Simulation, Verification and Validation) "L-H transition and pedestal physics" project (2019–2020) and TSVV "Plasma Particle/Heat Exhaust: Gyrokinetic/Kinetic Edge Codes" (2021–2025). It has received funding from the Euratom research and training programme 2014-2018 and 2019-2020 under grant agreement No 633053. The authors gratefully acknowledge funding from the European Commission Horizon 2020 research and innovation program under Grant Agreement No. 824158 (EoCoE-II). The views and opinions expressed herein do not necessarily reflect those of the European Commission. This research was supported in part by the National Science Foundation under Grant No. NSF PHY-1748958. We acknowledge PRACE for awarding us access to Joliot-Curie at GENCI@CEA, France and MareNostrum at Barcelona Supercomputing Center (BSC), Spain.

Data availability – The data that support the findings of this study are available upon request from the authors.

* guilhem.dif-pradalier@cea.fr

[1] P. H. Diamond and T. S. Hahm, On the dynamics of turbulent transport near marginal stability, Physics of Plasmas **2**, 3640 (1995).

[2] W. Thirring, Systems with negative specific heat, Zeitschrift für Physik A Hadrons and nuclei **235**, 339 (1970).

[3] R. S. Ellis, K. Haven, and B. Turkington, Large deviation principles and complete equivalence and nonequivalence results for pure and mixed ensembles, Journal of Statistical Physics **101**, 999 (2000).

[4] B. Saint-Michel, B. Dubrulle, L. Marié, F. Ravelet, and F. Daviaud, Evidence for forcing-dependent steady states in a turbulent swirling flow, Phys. Rev. Lett. **111**, 234502 (2013).

[5] D. E. Newman, B. A. Carreras, P. H. Diamond, and T. S. Hahm, The dynamics of marginality and self-organized criticality as a paradigm for turbulent transport, Physics of Plasmas **3**, 1858 (1996).

[6] X. Garbet and R. E. Waltz, Heat flux driven ion turbulence, Physics of Plasmas **5**, 2836 (1998).

[7] P. Beyer, S. Benkadda, X. Garbet, and P. H. Diamond, Nondiffusive transport in tokamaks: Three-dimensional structure of bursts and the role of zonal flows, Physical Review Letters **85**, 4892 (2000).

[8] B. F. McMillan, S. Jolliet, T. M. Tran, L. Villard, A. Bottino, and P. Angelino, Avalanchelike bursts in global gyrokinetic simulations, Physics of Plasmas **16**, 022310 (2009).

[9] Y. Idomura, H. Urano, N. Aiba, and S. Tokuda, Study of ion turbulent transport and profile formations using global gyrokinetic full-f Vlasov simulation, Nuclear Fusion **49**, 065029 (2009).

[10] Y. Sarazin, V. Grandgirard, J. Abiteboul, S. Allfrey, X. Garbet, P. Ghendrih, G. Latu, A. Strugarek, and G. Dif-Pradalier, Large scale dynamics in flux driven gyrokinetic turbulence, Nuclear Fusion **50**, 054004 (2010).

[11] R. Singh and P. H. Diamond, When does turbulence spreading matter?, Physics of Plasmas **27**, 042308 (2020), https://doi.org/10.1063/1.5117835.

[12] E. jin Kim and P. H. Diamond, Zonal flows and transient dynamics of the l-h transition, Physical Review Letters **90**, 10.1103/physrevlett.90.185006 (2003).

[13] P. H. Diamond, S.-I. Itoh, K. Itoh, and T. S. Hahm, Zonal flows in plasma—a review, Plasma Physics and Controlled Fusion **47**, 35 (2005).

[14] G. Dif-Pradalier, P. H. Diamond, V. Grandgirard, Y. Sarazin, J. Abiteboul, X. Garbet, P. Ghendrih, A. Strugarek, S. Ku, and C. S. Chang, On the validity of the local diffusive paradigm in turbulent plasma transport, Physical Review E **82**, 025401 (2010).

[15] G. Dif-Pradalier, G. Hornung, P. Ghendrih, Y. Sarazin, F. Clairet, L. Vermare, P. H. Diamond, J. Abiteboul, T. Cartier-Michaud, C. Ehrlacher, D. Estève, X. Garbet, V. Grandgirard, Ö. D. Gürcan, P. Hennequin, Y. Kosuga, G. Latu, P. Maget, P. Morel, C. Norscini, R. Sabot, and A. Storelli, Finding the elusive $\mathbf{E} \times \mathbf{B}$ staircase in magnetized plasmas, Physical Review Letters **114**, 10.1103/physrevlett.114.085004 (2015).

[16] F. Rath, A. G. Peeters, R. Buchholz, S. R. Grosshauser, P. Migliano, A. Weikl, and D. Strintzi, Comparison of gradient and flux driven gyro-kinetic turbulent transport, Physics of Plasmas **23**, 052309 (2016).

[17] A. G. Peeters, F. Rath, R. Buchholz, Y. Camenen, J. Candy, F. J. Casson, S. R. Grosshauser, W. A.

Hornsby, D. Strintzi, and A. Weikl, Gradient-driven flux-tube simulations of ion temperature gradient turbulence close to the non-linear threshold, Physics of Plasmas **23**, 082517 (2016).

[18] G. Dif-Pradalier, G. Hornung, X. Garbet, P. Ghendrih, V. Grandgirard, G. Latu, and Y. Sarazin, The $\mathbf{E}\times\mathbf{B}$ staircase of magnetised plasmas, Nuclear Fusion **57**, 066026 (2017).

[19] A. Ashourvan, R. Nazikian, E. Belli, J. Candy, D. Eldon, B. A. Grierson, W. Guttenfelder, S. R. Haskey, C. Lasnier, G. R. McKee, and C. C. Petty, Formation of a high pressure staircase pedestal with suppressed edge localized modes in the diii-d tokamak, Phys. Rev. Lett. **123**, 115001 (2019).

[20] M. Nakata and Y. Idomura, Plasma size and collisionality scaling of ion-temperature-gradient-driven turbulence, Nuclear Fusion **53**, 113039 (2013).

[21] R. Sanchez and D. E. Newman, Self-organized criticality and the dynamics of near-marginal turbulent transport in magnetically confined fusion plasmas, Plasma Physics and Controlled Fusion **57**, 123002 (2015).

[22] K. Ida, Z. Shi, H. J. Sun, S. Inagaki, K. Kamiya, J. E. Rice, N. Tamura, P. H. Diamond, G. Dif-Pradalier, X. L. Zou, K. Itoh, S. Sugita, O. D. Gürcan, T. Estrada, C. Hidalgo, T. S. Hahm, A. Field, X. T. Ding, Y. Sakamoto, S. Oldenbürger, M. Yoshinuma, T. Kobayashi, M. Jiang, S. H. Hahn, Y. M. Jeon, S. H. Hong, Y. Kosuga, J. Dong, and S.-I. Itoh, Towards an emerging understanding of non-locality phenomena and non-local transport, **55**, 013022.

[23] T. S. Hahm and P. H. Diamond, Mesoscopic transport events and the breakdown of fick's law for turbulent fluxes, Journal of the Korean Physical Society **73**, 747 (2018).

[24] D. P. G. Laval and J.-C. Adam, Wave-particle and wave-wave interactions in hot plasmas: a french historical point of view, The European Physical Journal H **43**, 421 (2018).

[25] E. V. A.A. Vedenov and R. Sagdeev, Quasilinear theory of plasma oscillations, Nuclear Fusion Supplement **2**, 465 (1962).

[26] W. Drummond and D. Pines, Nonlinear stability of plasma oscillations, Nuclear Fusion Supplement **3**, 1049 (1962).

[27] V. Grandgirard, J. Abiteboul, J. Bigot, T. Cartier-Michaud, N. Crouseilles, G. Dif-Pradalier, C. Ehrlacher, D. Esteve, X. Garbet, P. Ghendrih, G. Latu, M. Mehrenberger, C. Norscini, C. Passeron, F. Rozar, Y. Sarazin, E. Sonnendrücker, A. Strugarek, and D. Zarzoso, A 5D gyrokinetic full-f global semi-lagrangian code for flux-driven ion turbulence simulations, Computer Physics Communications **207**, 35 (2016).

[28] A. Peeters, Y. Camenen, F. Casson, W. Hornsby, A. Snodin, D. Strintzi, and G. Szepesi, The nonlinear gyro-kinetic flux tube code GKW, Computer Physics Communications **180**, 2650 (2009).

[29] C. Bourdelle, X. Garbet, F. Imbeaux, A. Casati, N. Dubuit, R. Guirlet, and T. Parisot, A new gyrokinetic quasilinear transport model applied to particle transport in tokamak plasmas, Physics of Plasmas **14**, 112501 (2007).

[30] J. Citrin, C. Bourdelle, F. J. Casson, C. Angioni, N. Bonanomi, Y. Camenen, X. Garbet, L. Garzotti, T. Görler, O. Gürcan, F. Koechl, F. Imbeaux, O. Linder, K. van de Plassche, P. Strand, and G. S. and, Tractable flux-driven temperature, density, and rotation profile evolution with the quasilinear gyrokinetic transport model QuaLiKiz, Plasma Physics and Controlled Fusion **59**, 124005 (2017).

[31] F. Jenko, W. Dorland, M. Kotschenreuther, and B. N. Rogers, Electron temperature gradient driven turbulence (AIP, 2000) pp. 1904–1910.

[32] M. Romanelli et al., Jintrac: A system of codes for integrated simulation of tokamak scenarios, Plasma and Fusion Research **9**, 3403023 (2014).

[33] J. B. Parker, L. L. LoDestro, and A. Campos, Investigation of a multiple-timescale turbulence-transport coupling method in the presence of random fluctuations, Plasma **1**, 126 (2018).

[34] X. Garbet, L. Laurent, A. Samain, and J. Chinardet, Radial propagation of turbulence in tokamaks, **34**, 963.

[35] Z. Lin and T. S. Hahm, Turbulence spreading and transport scaling in global gyrokinetic particle simulations, Physics of Plasmas **11**, 1099 (2004).

[36] T. S. Hahm, P. H. Diamond, Z. Lin, G. Rewoldt, Ö. D. Gürcan, and S. Ethier, On the dynamics of edge-core coupling, Physics of Plasmas **12**, 090903 (2005).

[37] G. Dif-Pradalier, E. Caschera, P. Ghendrih, Y. Asahi, P. Donnel, X. Garbet, V. Grandgirard, G. Latu, C. Norscini, and Y. Sarazin, Evidence for global edge–core interplay in fusion plasmas, Plasma and Fusion Research: Rapid Communications **12**, 10.1585/pfr.12.1203012.

[38] G. Dif-Pradalier, P. Ghendrih, Y. Sarazin, E. Caschera, F. Clairet, Y. Camenen, P. Donnel, X. Garbet, V. Grandgirard, Y. Munschy, L. Vermare, and F. Widmer, Transport barrier onset and edge turbulence shortfall in fusion plasmas, Communications Physics **5**, 229 (2022).

[39] F. Rath, A. G. Peeters, and A. Weikl, Analysis of zonal flow pattern formation and the modification of staircase states by electron dynamics in gyrokinetic near marginal turbulence, Physics of Plasmas **28**, 072305 (2021), https://doi.org/10.1063/5.0054358.

[40] L. Qi, M. Choi, J.-M. Kwon, and T. Hahm, Role of zonal flow staircase in electron heat avalanches in KSTAR l-mode plasmas, Nuclear Fusion **61**, 026010 (2021).

[41] A. Casati, C. Bourdelle, X. Garbet, F. Imbeaux,

J. Candy, F. Clairet, G. Dif-Pradalier, G. Falchetto, T. Gerbaud, V. Grandgirard, Özgur. D. Gürcan, P. Hennequin, J. Kinsey, M. Ottaviani, R. Sabot, Y. Sarazin, L. Vermare, and R. E. Waltz, Validating a quasi-linear transport model versus nonlinear simulations, Nuclear Fusion **49**, 085012 (2009).

[42] G. Dif-Pradalier, V. Grandgirard, Y. Sarazin, X. Garbet, and P. Ghendrih, Interplay between gyrokinetic turbulence, flows, and collisions: Perspectives on transport and poloidal rotation, Physical Review Letters **103**, 10.1103/physrevlett.103.065002 (2009).

[43] W. A. Houlberg, K. C. Shaing, S. P. Hirshman, and M. C. Zarnstorff, Bootstrap current and neoclassical transport in tokamaks of arbitrary collisionality and aspect ratio, Physics of Plasmas **4**, 3230 (1997), https://doi.org/10.1063/1.872465.

[44] Z. Lin, S. Ethier, T. S. Hahm, and W. M. Tang, Size scaling of turbulent transport in magnetically confined plasmas, Physical Review Letters **88**, 10.1103/PhysRevLett.88.195004 (2002).

[45] E. Caschera, Global confinement properties in global, flux-driven, gyrokinetic simulations, PhD thesis, Aix-Marseille Univ. (2019).

[46] A. M. Dimits, G. Bateman, M. A. Beer, B. I. Cohen, W. Dorland, G. W. Hammett, C. Kim, J. E. Kinsey, M. Kotschenreuther, A. H. Kritz, L. L. Lao, J. Mandrekas, W. M. Nevins, S. E. Parker, A. J. Redd, D. E. Shumaker, R. Sydora, and J. Weiland, Comparisons and physics basis of tokamak transport models and turbulence simulations, Physics of Plasmas **7**, 969 (2000).

[47] P. H. Diamond, S.-I. Itoh, and K. Itoh, *Modern Plasma Physics: Volume 1, Physical Kinetics of Turbulent Plasmas* (Cambridge University Press, 2010).

[48] N. Besse, Y. Elskens, D. F. Escande, and P. Bertrand, Validity of quasilinear theory: refutations and new numerical confirmation, Plasma Physics and Controlled Fusion **53**, 025012 (2011).

[49] R. A. Heinonen and P. H. Diamond, Subcritical turbulence spreading and avalanche birth, Physics of Plasmas **26**, 030701 (2019), https://doi.org/10.1063/1.5083176.

[50] S. Baschetti, H. Bufferand, G. Ciraolo, P. Ghendrih, E. Serre, P. Tamain, and the WEST Team, Self-consistent cross-field transport model for core and edge plasma transport, Nuclear Fusion **61**, 106020 (2021).

[51] X. Garbet, Y. Sarazin, F. Imbeaux, P. Ghendrih, C. Bourdelle, O. D. Gurcan, and P. H. Diamond, Front propagation and critical gradient transport models, Physics of Plasmas **14**, 122305 (2007), https://doi.org/10.1063/1.2824375.

[52] J. Dominski, S. Brunner, S. K. Aghdam, T. Görler, F. Jenko, and D. Told, Identifying the role of non-adiabatic passing electrons in itg/tem microturbulence by comparing fully kinetic and hybrid electron simulations, Journal of Physics: Conference Series **401**, 012006 (2012).